# Competing superfluid orders in spin-orbit-coupled fermionic cold-atom optical lattices

Yong Xu,[1] Chunlei Qu,[1] Ming Gong,[1,2] and Chuanwei Zhang[1,*]

[1]*Department of Physics, The University of Texas at Dallas, Richardson, Texas 75080, USA*
[2]*Department of Physics, The Chinese University of Hong Kong, Hong Kong*

The Fulde-Ferrell-Larkin-Ovchinnikov (FFLO) phase, a superconducting state with nonzero total momentum Cooper pairs in a large magnetic field, was first predicted about 50 years ago and has since become an important concept in many branches of physics. Despite an intensive search in various materials, unambiguous experimental evidence for the FFLO phase is still lacking in experiments. In this paper we show that both Fulde-Ferrell (FF) (a uniform order parameter with a plane-wave phase) and Larkin-Ovchinnikov (LO) phases (a spatially varying order parameter amplitude) can be observed using fermionic cold atoms in spin-orbit-coupled optical lattices. The increasing spin-orbit coupling enhances the FF phase over the LO phase. The coexistence of superfluid and magnetic orders is also found in the normal BCS phase. The pairing mechanism for different phases is understood by visualizing superfluid pairing densities in different spin-orbit bands. The possibility of observing similar physics using spin-orbit-coupled superconducting ultrathin films is also discussed.

## I. INTRODUCTION

The interplay between magnetism and superconductivity leads to various interesting phenomena, which have been intensively studied in many different materials [1–9]. The physics from such interplay can become even richer and more important when there exists strong spin-orbit (SO) coupling [10–12] in underlying physical systems, as evidenced by the recent impressive progress on the search for Majorana fermions using superconductor-semiconductor nanowire heterostructures [13–16]. Another well-known physics originating from the interplay between magnetism and superconductivity is the Fulde-Ferrell-Larkin-Ovchinnikov (FFLO) superconducting phase [1,2], where electrons form Cooper pairings with nonzero center-of-mass momentum in the presence of a large Zeeman field. In the past five decades, an intensive experimental search for FFLO phases has been done in different materials [6,7,17–20]. However, unambiguous experimental evidence for FFLO states is still elusive in experiments.

Ultracold degenerate Fermi gases may provide an ideal platform for exploring FFLO physics because of their intrinsic advantages such as the lack of orbital effects, being free of disorder, and having highly controllable experimental parameters. While previously FFLO phases have been widely studied in spin-imbalanced Fermi gases [21], the recent experimental realization of SO coupling for cold atoms [22] provides a completely different route for the experimental observation of FFLO phases. Note that there are two different types of FFLO phases: the FF (Fulde-Ferrell) state [1] with uniform amplitude but spatially dependent phase and the LO (Larkin-Ovchinnikov) [2] state with spatially oscillating amplitude but uniform phase of the order parameter.

In this paper we show that both the FF phase and a generalized LO phase may be observed in SO-coupled fermionic cold-atom optical lattices. Here the superfluid order parameters are obtained by self-consistently solving the real-

space Bogoliubov–de Gennes (BdG) equation. Without SO coupling, it is well known that LO states emerge in lattices with a large Zeeman field [23]. With SO coupling, FF phases have been proposed in free space without lattices [24–27], where the superfluid gap equation is solved in the momentum space (thus the spatial oscillation of the LO phase cannot be found). Our real-space BdG equation can capture both FF and LO phases and we show that there is a competition between them in a SO-coupled optical lattice [28,29]. Generally SO coupling enhances the FF phase but suppresses the LO phase. The generalized LO phase has no spatial nodes in the order parameter and magnetization, which is very different from traditional LO states in spin-imbalanced Fermi gases. The BCS pairing order also possesses finite magnetization, showing that the coexistence of magnetism and superfluid does not necessarily indicate the existence of FFLO phases [20]. The pairing mechanism for FF and LO phases is understood by visualizing the superfluid pairing densities in different SO bands. Finally, we discuss the possibility of observing similar physics using SO-coupled superconducting ultrathin films (e.g., Pb) [30–32].

## II. THEORETICAL MODEL

We consider fermionic cold atoms confined in a two-dimensional (2D) Rashba SO-coupled square optical lattice and subject to an in-plane Zeeman field. The system can be described by a Fermi-Hubbard Hamiltonian

$$H = H_0 + H_{SO} + H_Z, \tag{1}$$

where

$$H_0 = -t \sum_{\langle ij \rangle \sigma} \hat{c}_{i\sigma}^\dagger \hat{c}_{j\sigma} - \mu \sum_{i\sigma} \hat{n}_{i\sigma} + U \sum_i \hat{n}_{i\uparrow} \hat{n}_{i\downarrow} \tag{2}$$

is the usual single-particle Hamiltonian with an on-site interaction, $\hat{c}_{i\sigma}$ is the atom annihilation operator at the $i$th site with spin $\sigma$, and $\hat{n}_{i\sigma}$ is the particle number operator. Here $t$, $\mu$, and $U$ represent hopping strength, chemical potential,

---

*Corresponding author: chuanwei.zhang@utdallas.edu

and on-site interaction strength, respectively. In addition,

$$H_{SO} = -i\alpha \sum_{\langle ij \rangle} \hat{c}_i^\dagger (\mathbf{d}_{ij} \times \hat{\sigma} \cdot \mathbf{e}_z) \hat{c}_j \qquad (3)$$

is the Rashba SO coupling with $\hat{c}_i = (\hat{c}_{i\uparrow}\ \hat{c}_{i\downarrow})$, the Pauli matrix $\hat{\sigma}$, and the unit bond vector $\mathbf{d}_{ij}$ between nearest-neighbor sites $i$ and $j$, and

$$H_Z = h \sum_i (\hat{c}_{i\uparrow}^\dagger \hat{c}_{i\downarrow} + \hat{c}_{i\downarrow}^\dagger \hat{c}_{i\uparrow}) \qquad (4)$$

is an in-plane Zeeman field.

The superfluid phases can be studied under the standard mean-field approximation, where the on-site interaction can be decomposed as

$$U\hat{n}_{i\uparrow}\hat{n}_{i\downarrow} \approx \Delta_i^* \hat{c}_{i\downarrow}\hat{c}_{i\uparrow} + \Delta_i \hat{c}_{i\uparrow}^\dagger \hat{c}_{i\downarrow}^\dagger - |\Delta_i|^2/U + \text{HFC terms}. \qquad (5)$$

Here the order parameter $\Delta_i = U\langle \hat{c}_{i\downarrow}\hat{c}_{i\uparrow}\rangle$ and the Hartree-Fock correction (HFC) terms are $|n_{ix}|^2/U - n_{ix}\hat{c}_{i\downarrow}^\dagger \hat{c}_{i\uparrow} + n_{ix}^* \hat{c}_{i\uparrow}^\dagger \hat{c}_{i\downarrow} + U\langle \hat{n}_{i\uparrow}\rangle\hat{n}_{i\downarrow} + U\langle \hat{n}_{i\downarrow}\rangle\hat{n}_{i\uparrow} - U\langle \hat{n}_{i\uparrow}\rangle\langle \hat{n}_{i\downarrow}\rangle$ with $n_{ix} = U\langle \hat{c}_{i\uparrow}^\dagger \hat{c}_{i\downarrow}\rangle$. The mean-field Hamiltonian can be diagonalized by the Bogoliubov transformation $\hat{c}_{i\sigma} = \sum_{n=1}^{n=2N}(u_{i\sigma}^n \hat{\gamma}_n - \sigma v_{i\sigma}^{n*}\hat{\gamma}_n^\dagger)$ with quasiparticle operators $\hat{\gamma}_n$ and $\hat{\gamma}_n^\dagger$, yielding the BdG equation

$$\sum_j \begin{pmatrix} H_{ij} & \Delta_{ij} \\ \Delta_{ij}^* & -\sigma_y H_{ij}^* \sigma_y \end{pmatrix} \Phi_j^n = E_n \Phi_i^n, \qquad (6)$$

where $H_{ij}$ is a $2\times 2$ matrix with components $H_{ij}(\sigma\sigma) = -t\delta_{\langle ij \rangle} - \delta_{ij}\tilde{\mu}_{i\sigma}$, $H_{ij}(\uparrow\downarrow) = (h - n_{ix}^*)\delta_{ij} + i\alpha(\mathbf{d}_{ij} \times \hat{\sigma} \cdot \mathbf{e}_z)_{12}\delta_{\langle ij \rangle}$, and $H(\downarrow\uparrow) = H(\uparrow\downarrow)^*$. Here $\delta_{\langle ij \rangle} = 1$ for nearest neighbors and zero otherwise; $\tilde{\mu}_{i\sigma} = \mu - U\langle \hat{n}_{i\bar{\sigma}}\rangle$. The quasiparticle wave function $\Phi_j^n = (u_{j\uparrow}^n, u_{j\downarrow}^n, v_{j\downarrow}^n, v_{j\uparrow}^n)^T$. The BdG equation should be solved self-consistently with the atom density and pairing order parameter equations

$$\langle \hat{n}_{i\sigma}\rangle = \sum_{n=1}^{2N}[|u_{i\sigma}|^2 f(E_n) + |v_{i\sigma}|^2 f(-E_n)], \qquad (7)$$

$$n_{ix} = -U\sum_{n=1}^{2N}\{v_{i\uparrow}^n v_{i\downarrow}^{n*}[1 - f(E_n)] - u_{i\uparrow}^{n*}u_{i\downarrow}^n f(E_n)\}, \qquad (8)$$

$$\Delta_{ij} = -U\delta_{ij}\sum_{n=1}^{2N}\{u_{i\uparrow}^n v_{i\downarrow}^{n*}[1 - f(E_n)] - v_{i\uparrow}^{n*}u_{i\downarrow}^n f(E_n)\}. \qquad (9)$$

Here the Fermi-Dirac distribution $f(E_n) = 1/[1 + \exp(E_n/k_B T)]$. The ground-state energy is given by

$$\langle H \rangle = \sum_{n=1}^{2N} E_n \left[ f(E_n) - \sum_{i\sigma} |v_{i\sigma}^n|^2 \right] + \sum_i (|\Delta_i|^2/U + U\langle n_{i\uparrow}\rangle\langle n_{i\downarrow}\rangle - |n_{ix}|^2/U). \qquad (10)$$

In our numerical simulation, we choose different initial inputs of $\Delta_i$ and self-consistently solve the BdG equation (6) with a periodic boundary condition to calculate superfluid order parameters. If different phases are obtained for different
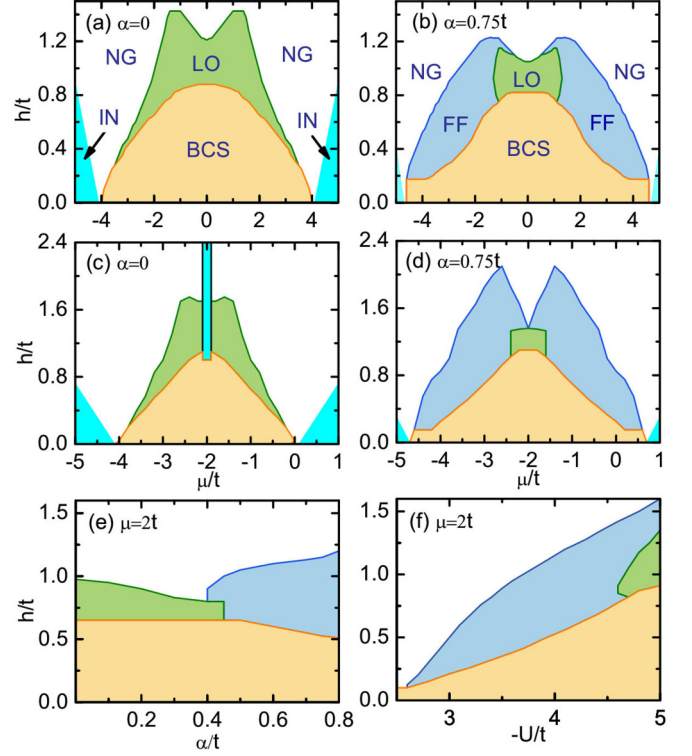


FIG. 1. (Color online) Mean-field phase diagrams as a function of chemical potential $\mu$ and Zeeman field $h$, (a) and (b) in the absence of HFC and (c) and (d) in the presence of HFC. (e) and (f) Phase diagrams (without HFC) with varying $\alpha$ and $U$ at $\mu = 2t$. We use a $16 \times 32$ square lattice with $U = -4t$ [except in (f)]; $T = 0$. (f) $\alpha = 0.75t$. BCS denotes uniform superfluid; NG, normal gas; and IN, insulator.

initial inputs, we compare the energies of these phases to determine the ground state.

## III. PHASE DIAGRAM

In Figs. 1(a)–1(d) we plot the zero-temperature mean-field phase diagram in the $(\mu,h)$ plane for $U = -4t$ without and with SO coupling. Here the parameters correspond to a typical set of parameters $t \sim 2$ KHz, $U \sim -8$ KHz, and $\alpha \sim 1.5$ KHz [33] in experiments, where $U$ and $\alpha$ can be tuned through Feshbach resonances [34] and coherent destructive tunneling methods [35], respectively. The phase diagram is symmetric about $\mu = 0$ and $\mu = -U/2$, respectively, for the cases without HFC and with HFC due to the particle-hole symmetry. Since the Zeeman field is along the $x$ direction, we can define the particle-hole operator $\mathcal{C}(\begin{smallmatrix}\hat{c}_{i\uparrow} \\ \hat{c}_{i\downarrow}\end{smallmatrix})\mathcal{C}^{-1} = e^{i\pi \cdot \mathbf{R}_i}(\begin{smallmatrix}\hat{c}_{i\downarrow}^\dagger \\ -\hat{c}_{i\uparrow}^\dagger\end{smallmatrix})$ and $\mathcal{C}(\begin{smallmatrix}\hat{c}_{i\uparrow}^\dagger \\ \hat{c}_{i\downarrow}^\dagger\end{smallmatrix})\mathcal{C}^{-1} = e^{-i\pi \cdot \mathbf{R}_i}(\begin{smallmatrix}\hat{c}_{i\downarrow} \\ -\hat{c}_{i\uparrow}\end{smallmatrix})$ with $\pi = (\pi,\pi)$ and $\mathcal{C}^2 = 1$. Under this transformation, $\mathcal{C}H(\mu)\mathcal{C}^{-1} = H(-\mu)$, leading to the symmetric phases about $\mu = 0$ observed in the numerical calculations. While in the presence of HFC, we have $\mathcal{C}H(\mu)\mathcal{C}^{-1} = H(-\mu - U)$ and the phase diagram is now symmetric about $\mu = -U/2$.

To distinguish different phases, we define the order parameter's amplitude variation $\sigma_1 = \sqrt{\sum_i (|\Delta_i| - \overline{|\Delta|})^2/N}$

with $\overline{|\Delta|} = \sum_i |\Delta_i|/N$ and phase variation $\sigma_2 = \sqrt{\sum_i |\Delta_i - \overline{\Delta}|^2/N}$ with $\overline{\Delta} = \sum_i \Delta_i/N$. The normal superfluid phase is characterized by $\overline{|\Delta|} \neq 0$, $\sigma_1 = \sigma_2 = 0$, the LO phase $\overline{|\Delta|} \neq 0$, and $\sigma_1 \neq 0$, while for the FF phase $\overline{|\Delta|} \neq 0$, $\sigma_1 = 0$, and $\sigma_2 = \overline{|\Delta|}$. Generally, a local superfluid order parameter can be written as $\Delta_i = \Delta_+ \exp(iyQ_y) + \Delta_- \exp(-iyQ_y + \phi)$, where $\phi$ is the relative phase between two $\pm\mathbf{Q}$ components. For normal superfluid phases $Q_y = 0$, while for LO and FF phases $Q_y \neq 0$. For LO phases both $\Delta_+$ and $\Delta_-$ are nonzero, while for FF phases one of them is zero. Note that both normal and insulator phases have $|\Delta| = 0$, but the excitations are gapless (gapped) for the normal (insulator) phase.

From Fig. 1(a) we see that without SO coupling, there is a large area of LO phase occupying the region with higher $h$ and no FF phase is found, which is consistent with the previous report [23]. However, in the presence of SO coupling [Fig. 1(b)], the FF phase emerges and its existence region is greatly enlarged with the increasing SO coupling. The region comes from the LO phase, the normal phase, and the BCS phase regions. This implies that the SO coupling enhances $h_{c2}$ for the transition to the normal phase [26,27] and reduces the $h_{c1}$ from BCS to FF phases. Furthermore, the LO region is reduced toward $\mu = 0$ (half filling). This is a clear competition between FF and LO phases in the presence of SO coupling, which is more explicitly shown in Fig. 1(e). With increasing SO coupling, the LO phase region becomes smaller, whereas the FF phase region becomes larger. Figure 1(f) shows the effects of interactions on the phase diagram. On the one hand, both BCS and FF phases are enhanced with increasing interactions; on the other hand, larger interactions are capable of inducing the LO phase.

In Figs. 1(c) and 1(d) we plot the phase diagram in the presence of HFC to show its effects. There is an insulator region around $\mu = -U/2$ without SO coupling, which is caused by the nesting of the Fermi surface. With SO coupling, the LO phase is decreased in the $\mu$ direction due to the effective chemical potential shift caused by the Hartree term, but increased in the $h$ direction compared to Fig. 1(b). The figure suggests that HFC only quantitatively changes the phase diagram. We also have confirmed that HFCs have no significant effects on the magnetization presented in Fig. 2. Therefore, we focus on the case without HFC in the following discussion.

Generally, traditional $s$-wave BCS pairings do not support finite magnetization because of equal contributions from both spins. The superfluid phases that support the coexistence of superfluidity and magnetism correspond to FFLO phases or Sarma phases [36,37], which are usually gapless. However, in the presence of SO coupling and a Zeeman field along the $x$ direction, a BCS pairing with gapped excitations also has a finite magnetization as observed in Figs. 2(a)–2(c). Figures 2(a) and 2(b) display, respectively, the phase transition from BCS states to FF states and from BCS states to LO states at certain parameter set points with a fixed SO coupling as the Zeeman field increases. The transition is manifested by the dramatic increases of the variations $\sigma_2$ and $\sigma_1$, respectively. We have also checked the Fourier transformation of the order parameter $\Delta$ and it shows that apart from nonzero $Q_y$, $\Delta_+ \neq 0$ and $\Delta_- = 0$ for the FF phase, while neither vanishes for the
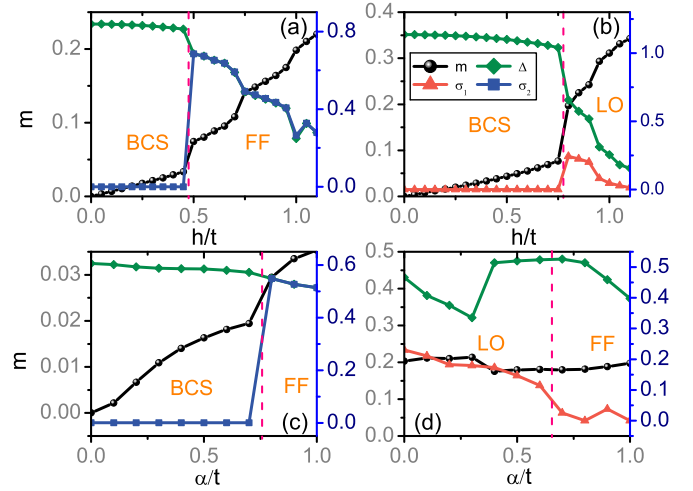


FIG. 2. (Color online) Change of the average order parameter $\Delta$ (diamond green line), magnetization $m$ (circle black line) defined as $m = \sum_i \langle \hat{m}_i \rangle / N$ with $\hat{m}_i = \hat{c}_{i\uparrow}^\dagger \hat{c}_{i\downarrow} + \hat{c}_{i\downarrow}^\dagger \hat{c}_{i\uparrow}$, amplitude variation $\sigma_1$ (triangle red line), and phase variation $\sigma_2$ (square blue line) across the phase transitions, for (a) and (b) $\alpha = 0.75t$ with (a) $\mu = -2t$, (b) $\mu = -0.4t$, (c) $\mu = -3t$ and $h = 0.3t$, and (d) $\mu = -1.5t$ and $h = 0.9t$. The left vertical axis is for $m$, while the right axis is for $\Delta$, $\sigma_1$, and $\sigma_2$. The vertical pink lines indicate the phase transition points. The unit of $\Delta$, $\sigma_1$, and $\sigma_2$ is $t$.

LO phase. The phase variation of the FF state can also be seen from the fact that $\sigma_2$ is equal to $\Delta$. Figures 2(c) and 2(d) show the transition from BCS to FF phases and from LO to FF phases at certain points with a fixed Zeeman field as the SO coupling $\alpha$ is increased, indicating the growth of FF phases and the suppression of BCS and LO phases by the SO coupling. Around the transition point from LO to FF phases, there is no clear change of the magnetization. The kink of $\Delta$ around $\alpha = 0.3$ in Fig. 2(d) (not at the phase transition point) is caused by the change of periodicity of $\Delta$ in the LO phase.

## IV. REAL-SPACE SIGNATURES

Previously the LO phase in lattice models was generally characterized by an inhomogeneous real order parameter and the existence of domain walls at the node points $\Delta_i = 0$ that contain the largest magnetization [23,38]. These results are reproduced in our calculation without SO coupling. However, when SO coupling is included, $\Delta_i$ is no longer real in the LO phase and does not contain nodes, as clearly seen from Fig. 3(b). The real and imaginary parts of the order parameter have different phase and amplitude (i.e., $\Delta_+ \neq \Delta_-$) [Fig. 3(a)], indicating that the order parameter has both phase and amplitude variations, which are very different from traditional FF or LO phases. Such nonzero $\Delta_i$ is caused by the imbalance between the pairings with momentum $\pm\mathbf{Q}$, which will be explained in detail in the next section. The magnetization $m$ also oscillates in space and reaches the maximum at the minimum of the absolute $|\Delta|$ [see Fig. 3(b)]. In the FF phase $\Delta_i = \Delta_0 \exp(iyQ_y)$, hence the phase varies, but the magnitude of the order parameter and the magnetization are uniform, as shown in Figs. 3(c) and 3(d). The Fourier transformation of
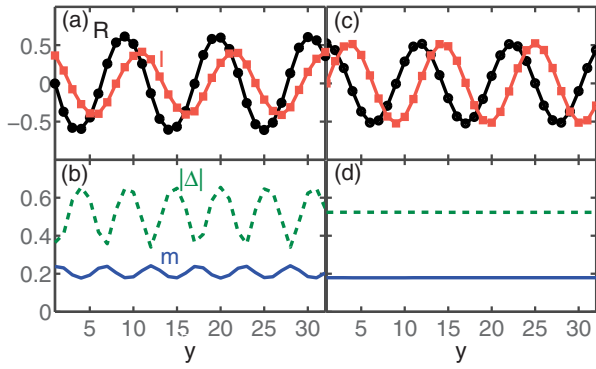
FIG. 3. (Color online) Order parameter and magnetization in real space along the $y$ direction for (a) and (b) the generalized LO phase with $\alpha = 0.75t$, $\mu = -1.2t$, and $h = 0.9t$ and (c) and (d) the FF phase with $\alpha = 0.75t$, $\mu = -1.5t$, and $h = 0.9t$. The circle black and square red lines correspond to the real and imaginary parts of $\Delta$ with the unit $t$.

the order parameters shows two peaks at $\pm\mathbf{Q}$ for the LO phase, but one peak at $\mathbf{Q}$ for the FF phase, as expected.

## V. PAIRING MECHANISM

It is natural to ask why the combination of SO coupling and an in-plane Zeeman field is capable of enhancing the parameter region for the FF pairing while suppressing that for the LO pairing. This can be understood from different pairing densities of these two phases. We find that in the former, the pairing mainly occurs around the Fermi surface lying at the lower energy band in the helicity representation, while in the latter, the pairing occurs at both energy bands. Figure 4(a) illustrates the single-particle band structure at a typical FF phase point with $\alpha = 0.75t$, $\mu = -3t$, and $h = 0.6t$. The Fermi surface is plotted at the bottom of the box with green lines. It is clearly seen that an in-plane Zeeman field with SO coupling leads to the asymmetric Fermi surface around the origin along the $y$ direction, i.e., the lower band (denoted as $-$) has the lowest energy state located at positive $k_y$ and the upper band (denoted as $+$) at negative $k_y$. Cooper pairings with approximately opposite spins happen mainly around the Fermi surface of the lower band as shown in Fig. 4(b) due to its higher density of states compared with the upper one. The deformation of the Fermi surface finally leads to the finite center-of-mass momentum of Cooper pairs.

As shown in Fig. 1(b), when the chemical potential ($\mu < 0$) is increased, the system enters into the BCS superfluid region from the FF region resulting from the decreased deformation of the Fermi surface. However, for certain larger Zeeman fields, the same manipulation drives the system to the LO phase. In this phase, primary contributions to Cooper pairs are from fermions not only around the Fermi surface of the lower band, but also around that of the higher band as the pairing density shows in Fig. 4(c). Since these pairs from different bands have opposite momenta, the amplitude of the resulting order parameter has a spatial oscillation structure. In contrast to traditional LO phases, the imbalance (that is, $\Delta_+ \neq \Delta_-$) of the numbers of pairings with opposite momenta leads to the absence of nodes, giving the generalized LO phase. It can be
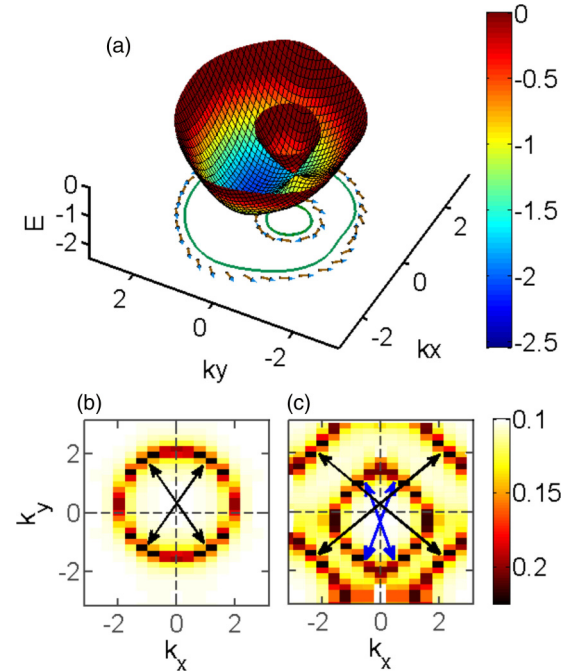


FIG. 4. (Color online) (a) Single-particle band structure in the momentum space with $\alpha = 0.75t$, $h = 0.6t$, and $\mu = -3.0t$. The Fermi surface is plotted on the bottom layer with the green line. The small arrows around the Fermi surface are the spin orientations. (b) Pairing density $|\langle \hat{c}_{\mathbf{k},-} \hat{c}_{-\mathbf{k}+Q_y,-}\rangle|^2$ with $Q_y = 3\pi/16a$ and lattice constant $a$, where $-$ indicates the lower branch. The black double arrows show the pairing. The parameters are the same as in (a). (c) Pairing densities $|\langle \hat{c}_{\mathbf{k},-} \hat{c}_{-\mathbf{k}+Q_y,-}\rangle|^2$ and $|\langle \hat{c}_{\mathbf{k},+} \hat{c}_{-\mathbf{k}-Q_y,+}\rangle|^2$ for the LO phase with $\alpha = 0.75t$, $h = 0.85t$, and $\mu = -0.2t$. Here $+$ indicates the higher branch. The black and blue double arrows illustrate the Cooper pairings with $Q_y$ and $-Q_y$, respectively; $Q_y$ depends on the deformation of the Fermi surface by the SO coupling and the Zeeman field. The units of $E$ and $k_x, k_y$ are $t$ and $1/a$, respectively.

seen that the pairing mechanism is very different from the case without SO coupling, where pairing happens at different bands. In this case, if there is a nonzero momentum pairing, there is always another pairing with the opposite momentum to lower the energy [23]. The consequence is the absence of the FF phase and the presence of the LO phase with nodes.

## VI. EXPERIMENTAL OBSERVATION

In experiments, the Rashba SO coupling and an in-plane Zeeman field in a square lattice can be realized using six lasers that couple two different hyperfine ground states of atoms [39]. Since we are mainly interested in the superfluid phase, only a weak optical lattice is needed. For a typical set of parameters $t \sim 2$ KHz, $U \sim -8$ KHz, and $\alpha \sim 1.5$ KHz [33], the resulting pairing order $\Delta \sim 1$ KHz $\sim 50$ nK, which could be further enhanced by increasing the interaction through a Feshbach resonance. The critical Zeeman field is generally on the order of 0.5 KHz. These parameters show that the FFLO phases should be observable with a reasonably low temperature and realistic experimental setup. In experiments, the magnetization and the pairing order strength can be observed in the standard spin-resolved time-of-flight image,

while the finite center-of-mass momentum of the Cooper pairs may be observed using noise-correlation method or momentum-resolved radio-frequency spectroscopy [25]. In previous spin-imbalanced Fermi gases, the observation of the coexistence of superfluid and magnetism is generally taken as a signature of the FFLO phase [20]. However, it is no longer true in our case because a BCS phase also has finite magnetization. In order to observe the FFLO phase, one should detect the pairing momentum or the magnetization oscillation in the LO phase directly.

## VII. POSSIBLE OBSERVATION IN SO-COUPLED SUPERCONDUCTING THIN FILMS

Finally, we remark that the same physics may also be observed using SO-coupled $s$-wave ultrathin superconducting films subject to an in-plane Zeeman field, which may be realized using an in-plane magnetic field or a magnetic semiconductor substrate. Recently, superconductivity in the extreme 2D limit (down to two atomic layers) has been observed in experiments for many materials [30]. In some of these thin films, such as Pb, strong Rashba spin-orbit coupling exists and can be tuned through a variable Schottky barrier [31]. Furthermore, the $H_{c2}$ critical field for these materials can be extremely large for an in-plane magnetic field [32]. Such spin-orbit-coupled ultrathin superconducting films allow for the possible observation of FFLO phases, which is similar to the

role of semiconductor-superconductor nanoheterostructures for the recent search of Majorana fermions [13–15]. In Pb experiments, a typical set of parameters is $t \sim 40$ meV and $\alpha \sim 17$ meV. However, the interaction $U$ is generally much weaker, leading to an experimentally observed $s$-wave order parameter $\Delta \sim 0.7$ meV (which corresponds to the Pb thin-film superconducting transition temperature $T_c = 6$ K). The required Zeeman field for the phase transition $h < \Delta$, which requires a magnetic field $B < 6$ T for a small $g$ factor $g = 2$, which is below the upper critical magnetic field $B \sim 8$ T. In the thin films, the FFLO vector $Q \propto h_x$ is much smaller due to the small deformation of the Fermi surface by a small Zeeman field and the resulting order parameter oscillation period should be much longer. In experiments, the local order parameter minima in the LO state can accommodate normal quasiparticles, which lead to nonzero differential conductance that can be detected through local tunneling measurement. In addition, the Josephson junction between a FFLO superconductor and a conventional BCS superconductor [40] can also be used to detect the FFLO phases.

[1] P. Fulde and R. A. Ferrell, Phys. Rev. **135**, A550 (1964).

[2] A. I. Larkin and Yu. N. Ovchinnikov, Zh. Eksp. Teor. Fiz. **47**, 1136 (1964) [Sov. Phys. JETP **20**, 762 (1965)].

[3] W. E. Pickett, R. Weht, and A. B. Shick, Phys. Rev. Lett. **83**, 3713 (1999).

[4] J. W. Lynn, B. Keimer, C. Ulrich, C. Bernhard, and J. L. Tallon, Phys. Rev. B **61**, R14964 (2000).

[5] S. S. Saxena *et al.*, Nature (London) **406**, 587 (2000).

[6] M. Kenzelmann *et al.*, Science **321**, 1652 (2008).

[7] L. Li, C. Richter, J. Mannhart, and R. C. Ashoori, Nat. Phys. **7**, 762 (2011).

[8] J. A. Bert *et al.*, Nat. Phys. **7**, 767 (2011).

[9] D. A. Dikin, M. Mehta, C. W. Bark, C. M. Folkman, C. B. Eom, and V. Chandrasekhar, Phys. Rev. Lett. **107**, 056802 (2011).

[10] D. Xiao, M.-C. Chang, and Q. Niu, Rev. Mod. Phys. **82**, 1959 (2010).

[11] M. Z. Hasan and C. L. Kane, Rev. Mod. Phys. **82**, 3045 (2010).

[12] I. Žutić, J. Fabian, and S. Das Sarma, Rev. Mod. Phys. **76**, 323 (2004).

[13] V. Mourik, K. Zuo, S. M. Frolov, S. R. Plissard, E. P. A. M. Bakkers, and L. P. Kouwenhoven, Science **336**, 1003 (2012).

[14] M. T. Deng, C. L. Yu, G. Y. Huang, M. Larsson, P. Caroff, and H. Q. Xu, Nano Lett. **12**, 6414 (2012).

[15] A. Das, Y. Ronen, Y. Most, Y. Oreg, M. Heiblum, and H. Shtrikman, Nat. Phys. **8**, 887 (2012).

[16] L. P. Rokhinson, X. Liu, and J. K. Furdyna, Nat. Phys. **8**, 795 (2012).

[17] H. A. Radovan, N. A. Fortune, T. P. Murphy, S. T. Hannahs, E. C. Palm, S. W. Tozer, and D. Hall, Nature (London) **425**, 51 (2003);

A. Bianchi, R. Movshovich, C. Capan, P. G. Pagliuso, and J. L. Sarrao, Phys. Rev. Lett. **91**, 187004 (2003); K. Kakuyanagi, M. Saitoh, K. Kumagai, S. Takashima, M. Nohara, H. Takagi, and Y. Matsuda, *ibid.* **94**, 047602 (2005); Y. Matsuda and H. Shimahara, J. Phys. Soc. Jpn. **76**, 051005 (2007).

[18] S. Uji *et al.*, Phys. Rev. Lett. **97**, 157001 (2006); R. Lortz, Y. Wang, A. Demuer, P. H. M. Böttger, B. Bergk, G. Zwicknagi, Y. Nakazawa, and J. Wosnitza, *ibid.* **99**, 187002 (2007); B. Bergk, A. Demuer, I. Sheikin, Y. Wang, J. Wosnitza, Y. Nakazawa, and R. Lortz, Phys. Rev. B **83**, 064506 (2011); W. A. Coniglio, L. E. Winter, K. Cho, C. C. Agost, B. Fravel, and L. K. Montgomery, *ibid.* **83**, 224507 (2011).

[19] K. Cho, H. Kim, M. A. Tanatar, Y. J. Song, Y. S. Kwon, W. A. Coniglio, C. C. Agosta, A. Gurevich, and R. Prozorov, Phys. Rev. B **83**, 060502(R) (2011).

[20] Y.-A. Liao, A. S. C. Rittner, T. Paprotta, W. Li, G. B. Partridge, R. G. Hulet, S. K. Baur, and E. Mueller, Nature (London) **467**, 567 (2010).

[21] H. Hu and X.-J. Liu, Phys. Rev. A **73**, 051603(R) (2006); L. He, M. Jin, and P. Zhuang, Phys. Rev. B **74**, 024516 (2006); M. M. Parish, F. M. Marchetti, A. Lamacraft, and B. D. Simons, Nat. Phys. **3**, 124 (2007); M. Iskin and C. A. R. Sá de Melo, Phys. Rev. Lett. **97**, 100404 (2006); D. E. Sheehy, Ann. Phys. (NY) **322**, 1790 (2007); A. Bulgac and M. M. Forbes, Phys. Rev. Lett. **101**, 215301 (2008); T. K. Koponen, T. Paananen, J.-P. Martikainen, and P. Törmä, *ibid.* **99**, 120403 (2007); E. Zhao and W. V. Liu, Phys. Rev. A **78**, 063605 (2008); Y. Okawauchi and A. Koga, J. Phys. Soc. Jpn. **81**, 074001 (2012); J. P. A. Devreese, S. N. Klimin, and J. Tempere, Phys. Rev. A **83**, 013606 (2011);

J. P. A. Devreese, M. Wouters, and J. Tempere, *ibid.* **84**, 043623 (2011).

[22] Y.-J. Lin, K. Jiménez-García, and I. B. Spielman, Nature (London) **471**, 83 (2011); J.-Y. Zhang *et al.*, Phys Rev. Lett. **109**, 115301 (2012); C. Qu, C. Hamner, M. Gong, C. Zhang, and P. Engels, Phys. Rev. A **88**, 021604(R) (2013); P. Wang, Z.-Q. Yu, Z. Fu, J. Miao, L. Huang, S. Chai, H. Zhai, and J. Zhang, Phys. Rev. Lett. **109**, 095301 (2012); L. W. Cheuk, A. T. Sommer, Z. Hadzibabic, T. Yefsah, W. S. Bakr, and M. W. Zwierlein, *ibid.* **109**, 095302 (2012).

[23] Y. L. Loh and N. Trivedi, Phys. Rev. Lett. **104**, 165302 (2010).

[24] Z. Zheng, M. Gong, X. Zou, C. Zhang, and G. Guo, Phys. Rev. A **87**, 031602(R) (2013); F. Wu, G.-C. Guo, W. Zhang, and W. Yi, Phys. Rev. Lett. **110**, 110401 (2013); Z. Zheng, M. Gong, Y. Zhang, X. Zou, C. Zhang, and G. Guo, arXiv:1212.6826; X.-J. Liu and H. Hu, Phys. Rev. A **87**, 051608(R) (2013); L. Dong, L. Jiang, and H. Pu, New J. Phys. **15**, 075014 (2013); H. Hui and X.-J. Liu, *ibid.* **15**, 093037 (2013); X.-J. Liu, Phys. Rev. A **88**, 043607 (2013).

[25] Z. Fu, L. Huang, Z. Meng, P. Wang, X.-J. Liu, H. Pu, H. Hu, and J. Zhang, Phys. Rev. A **87**, 053619 (2013).

[26] V. Barzykin and L. P. Gor'kov, Phys. Rev. Lett. **89**, 227002 (2002).

[27] K. Michaeli, A. C. Potter, and P. A. Lee, Phys. Rev. Lett. **108**, 117003 (2012).

[28] C. Qu, M. Gong, and C. Zhang, arXiv:1304.3926.

[29] M. Iskin, Phys. Rev. A **88**, 013631 (2013).

[30] T. Zhang *et al.*, Nat. Phys. **6**, 104 (2010).

[31] B. Slomski, G. Landolt, G. Bihlmayer, J. Osterwalder, and J. H. Dil, Sci. Rep. **3**, 1963 (2013).

[32] H. J. Gardner, A. Kumar, L. Yu, P. Xion, M. P. Warusawithana, L. Wang, O. Vafek, and D. G. Schlom, Nat. Phys. **7**, 895 (2011).

[33] M. Gong, Y. Qian, V. W. Scarola, and C. Zhang, arXiv:1205.6211.

[34] C. Chin, R. Grimm, P. Julienne, and E. Tiesinga, Rev. Mod. Phys. **82**, 1225 (2010).

[35] Y. Zhang, G. Chen, and C. Zhang, Sci. Rep. **3**, 1937 (2013).

[36] G. Sarma, J. Phys. Chem. Solids **24**, 1029 (1963).

[37] W. V. Liu and F. Wilczek, Phys. Rev. Lett. **90**, 047002 (2003).

[38] Q. Cui and K. Yang, Phys. Rev. B **78**, 054501 (2008).

[39] X.-J. Liu, K. T. Law, and T. K. Ng, arXiv:1304.0291.

[40] K. Yang and D. F. Agterberg, Phys. Rev. Lett. **84**, 4970 (2000).